Journal of Medicinal Chemistry

Article

pubs.acs.org/jmc

Inhibition of Glutathione *S*-Transferase M1 by New Gabosine Analogues Is Essential for Overcoming Cisplatin Resistance in Lung Cancer Cells

Chie-Hong Wang,[†] Ho T. Wu,[‡] Hau M. Cheng,[‡] Tien-Jui Yen,[†] I-Hsuan Lu,[†] Hui Chuan Chang,[†] Shu-Chuan Jao,[§] Tony K. M. Shing,*[,‡] and Wen-Shan Li*[,†,∥]

[†]Institute of Chemistry, Academia Sinica, Taipei 115, Taiwan

[‡]Department of Chemistry and Center of Novel Functional Molecules, The Chinese University of Hong Kong, Shatin, Hong Kong, China

[§]Institute of Biological Chemistry, Academia Sinica, Taipei 115, Taiwan

[∥]Doctoral Degree Program in Marine Biotechnology, National Sun Yat-Sen University, Kaohsiung 804, Taiwan

Supporting Information

ABSTRACT: A new class of human GST inhibitors has been identified via rational design approach; we report their discovery, synthesis, inhibitory activity, and synergetic effect in combination with cisplatin against A549 lung cancer cell line. The results of this effort show that the lead 4-*O*-decyl-gabosine D (**24**) has optimum synergetic effect in A549 human lung adenocarcinoma epithelial cell and that this activity involves inhibition of glutathione *S*-transferase M1, apparently consistent with siRNA-mediated knockdown of GSTM1 gene.

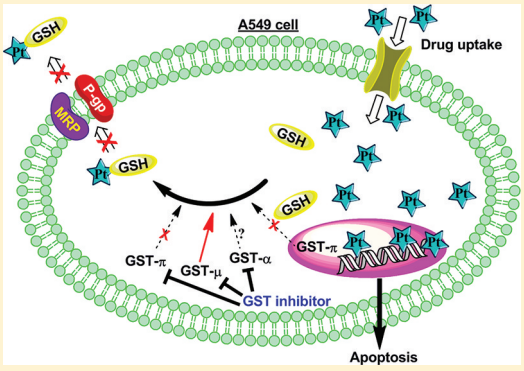

INTRODUCTION

Human glutathione *S*-transferases (hGSTs), a family of GSH-dependent enzymes in phase II detoxification system, participate in drug resistance processes by catalyzing the conjugation of glutathione (GSH) to a wide variety of anticancer drugs (e.g., cisplatin, oxaliplatin, thiotepa, chlorambucil, melphalan, cyclophosphamide, doxorubicin, and so on).[1] The resulting GS−drug conjugates are more hydrophilic and are eliminated from the cell through transporter proteins, multidrug-resistance-related proteins (MRP) and P-glycoprotein (P-gp).[2] This operating mechanism elevates the efflux activity of drugs in cancer cells, resulting in anticancer drug resistance (Figure 1).[3] To date, traditional GST inhibitors are customarily considered to be used with anticancer drugs for cancer patients to prevent multidrug resistance occurrence. Consequently, investigations and development on GST inhibitors would have practical applications in chemoresistance.

Eight classes of GSTs in mammals have been identified on the basis of their biofunctional properties and sequence identities.[4] Among these GST isoenzymes, GST P1-1, GST A2, and GST M1 are overexpressed in many cancer cell lines including breast, lung, and ovarian cancers.[5] There are two main types of GST inhibitors: non-GSH compounds[6] and GSH analogues.[7] Although diverse GST inhibitors have been identified by several distinctive strategies, they are classically

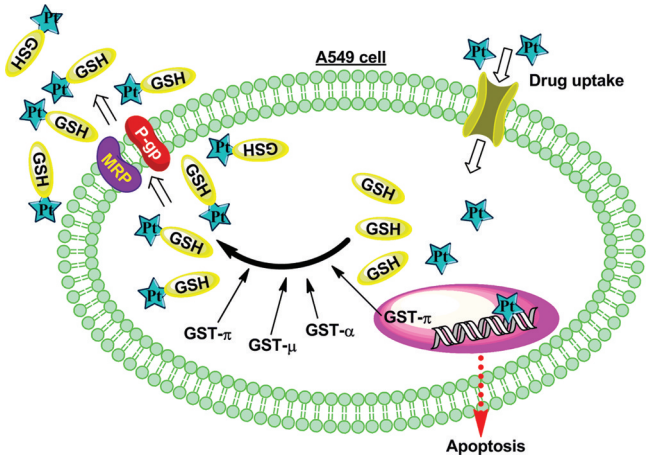

Figure 1. Possible GST-mediated activation of anticancer drug resistance in lung cancer cells.

restricted to GSH−ethacrynic acid derivatives with poor cell membrane permeability. Gabosines, a family of multihydroxylated cyclohexenones and cyclohexanones,[8] have been developed

Received: August 24, 2011
Published: November 15, 2011

and synthesized previously in our group.[9] In particular, some gabosines have been demonstrated to exhibit biological applications such as antibiotics, anticancer agents, and DNA intercalating agents,[10] thereby inspiring us to pursue research on the capability of gabosine analogues on GST inhibition. Herein we report a rapid discovery of new GST inhibitors via rational design strategy and identify the capability of 4-*O*-decyl-gabosine D (**24**) to suppress the resistance against cisplatin in lung cancer cells by inhibiting GSTM1.

RESULT AND DISCUSSION

Gabosines G (**1**)[9a] and D (**3**)[9b] were prepared as reported previously (Figure 2). The syntheses of 4-*epi*-gabosine D (**2**)

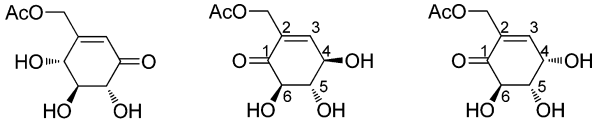

Figure 2. Structures of gabosine analogues **1**–**3**.

and analogues **4**–**24** are briefly summarized in Scheme 1 (see Supporting Information for details). The known enone **4** was made from D-glucose via a key intramolecular direct aldol reaction of a diketone derived from D-glucose.[9c] Deacetonation of **4** under mild acid hydrolysis gave diol **5**, which was regioselectively esterified to yield acetate **6**. Enone **4** was stereoselectively reduced by sodium borohydride or K-selectride to give known β-allylic alcohol **25**[9c] or α-allylic alcohol **26**,[9b] respectively. Alkylation of the free alcohol in **25** and **26** afforded the corresponding ethers **27** and **28**, which were converted into respective enones **10**, **11**, and **15**–**23** in three steps involving deacetonation, regioselective acetylation, and pyridinium dichromate (PDC) oxidation. Acid hydrolysis of the *trans*-diacetal goup in **10**, **11**, **15**, **16**, and **23** furnished enone-diols **7**, **8**, **12**, **13**, and **24**, respectively. *tert*-Butyldimethylsilylation of **25** and **26** afforded silyl ethers **29** and **30**, which underwent deacetonation, regioselective acetylation, oxidation, and desilylation to give enone-alcohol **9** and **14**, respectively. Acidic removal of the trans-diacetal group in **9** gave 4-*epi*-gabosine D (**2**).

To date, ethacrynic acid with a Michael acceptor, and some of its analogues have been demonstrated to effectively inhibit various GSTs.[1b,11,7c] There are two possible mechanisms for inhibition of GST isozymes: formations of the enzyme–ethacrynic acid adduct[1b] and GS–ethacrynic acid conjugate.[1b,7c] Because gabosine, bearing the trihydroxycyclohexenone skeleton with a reactive Michael acceptor, represents a promising core structure, we chose it as the key compound for the development of GST inhibitors.

Scheme 1. Syntheses of Gabosine Analogues

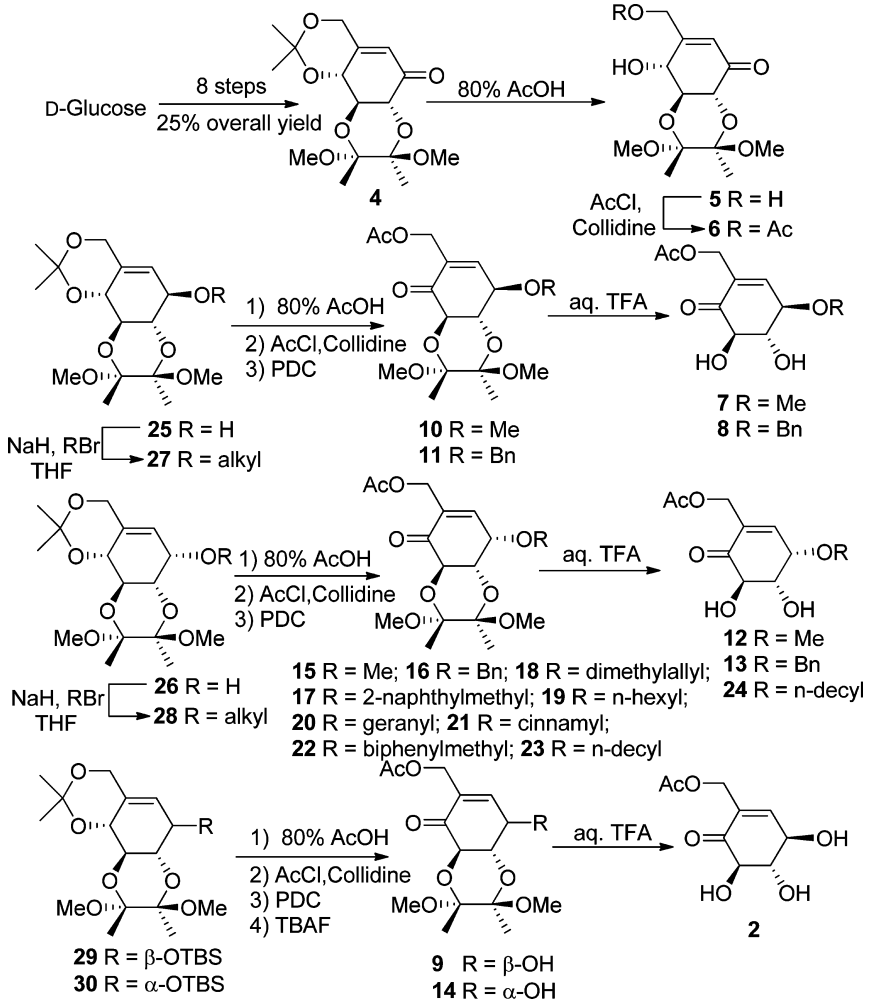

dx.doi.org/10.1021/jm201131n | J. Med. Chem. 2011, 54, 8574–8581

In the initial screening of gabosine analogues, we identified that gabosines **1**−**3** (Figure 2) could abolish GSTA2 and GSTP1-1 activities (Table 1, IC_{50} > 75 and >100 μM, respectively). To enhance the potency of enones **1**−**3**, we initially designed and synthesized 13 compounds **4**−**16** with appropriately protected hydroxy units and methyl/benzyl ether moieties that had been selected to modulate hydrophobicity (Figure 3 and Scheme 1). This exercise to improve the IC_{50} was successful. For example, alcohol **14** and methyl ether **15**, gabosine D (**3**) analogues, showed an acceptable inhibitory activity against GSTP1-1 with IC_{50} values of 82.5 and 62.7 μM, respectively (Table 1). Similarly, benzyl-diol **8** and benzyl-diacetal **11** (IC_{50} = 24.7 and 24.5 μM), 4-*epi*-gabosine D (**2**) analogues, exhibited a 2−3-fold potency increase over **14** and **15**. Furthermore, benzyl-diol **13** and benzyl-diacetal **16**, the 4-epimers of **8** and **11**, respectively, were found to have IC_{50} values of 16.3 and 20.2 μM, representing 4−5-fold higher potency than **14** and **15**. In contrast, this series displayed weak inhibitory activity against human GSTA2. Collectively, the results show that the presence of a methoxy or benzyloxy substituent in gabosine (especially for gabosine D) at C-4 leads to significantly enhanced efficacy against GSTP1-1, suggesting perhaps that a hydrophobic moiety at position 4 could occupy a hydrophobic region in the active site pocket of the enzyme. Building on these observations, we therefore searched for hydrophobic moieties that can improve structure activity profiles.

Thus, seven analogues (**17**−**23**) related to benzyl-diacetal **16** (one of the most active compounds) with systematic variations of the C-4 ether moiety were prepared (Figure 3, Scheme 1 and Figure 4). Among these analogues (Table 1 and Table 2), enone **23** with a decyl ether group was the most active one with respective IC_{50} values of 33.1, 33.6, and 36.5 μM toward GSTA2, GSTM1, and GSTP1-1. Acid hydrolysis of diacetal-enone **23** was achieved to give diol-enone **24**, which showed a potent inhibitory activity against GSTM1, with an IC_{50} value of 13.4 μM, and a similar inhibitory potency toward GSTA2 and GSTP1-1 (IC_{50} = 37.8 and 25.3 μM, respectively). Because the overexpression of different GSTs in tumor cells is known, this has spawned the development of new chemical entity to inhibit multiple GST isozymes. 4-*O*-Decyl-gabosine D (**24**) represents an example of a promising new class of potent human GST inhibitors and is used in this study.

Table 1. Inhibitory Constants of Gabosine Analogues 1−20 against different GST Isozymes[a]

	inhibitory activity, IC_{50} (μM)		
compd	GSTA2	GSTM1	GSTP1−1
1	>100 (18)[b]	[c]	>100 (20)[b]
2	>100 (27)[b]	[c]	>100 (25)[b]
3	>100 (12)[b]	[c]	>100 (11)[b]
4	>100 (16)[b]	[c]	>100 (15)[b]
5	>100 (19)[b]	[c]	[c]
6	>100 (17)[b]	[c]	>100 (7)[b]
7	>100 (16)[b]	[c]	>100 (23)[b]
8	>100 (20)[b]	[c]	24.7 ± 2.1
9	>100 (15)[b]	[c]	>100 (16)[b]
10	>100 (16)[b]	[c]	>100 (38)[b]
11	[c]	[c]	24.5 ± 1.7
12	>100 (16)[b]	[c]	>100 (12)[b]
13	>100 (14)[b]	[c]	16.3 ± 1.9
14	[c]	[c]	82.5 ± 5.3
15	[c]	[c]	62.7 ± 8.4
16	>100 (10)[b]	[c]	20.2 ± 0.8
17	77.6 ± 4.4	56.6 ± 9.2	48.2 ± 4.2
18	96.3 ± 5.2	162.7 ± 52.1	37.6 ± 6.3
19	93.0 ± 2.9	123.5 ± 16.1	52.4 ± 6.6
20	178.6 ± 23.2	176.7 ± 25.8	179.0 ± 29.1

[a]Inhibitor concentration at which half-maximal enzyme activity is obtained (IC_{50}, mean ± SEM, n = 3). [b]The percent (%) inhibition, in parentheses, at 100 μM is expressed as the percent (%) inhibition of enzyme activity without correction for the contribution of the formation of glutathione conjugate. [c]Not determined.

For inhibition characteristics toward GSTM1, steady-state kinetic analysis showed that **24** was competitive versus GSH (K_i = 3.2 μM) but was noncompetitive versus CDNB (K_i = 4.7 μM; Table 2 and Figure 5). These results indicate that inhibitor **24** competes with GSH for the hydrophilic binding site (G-site), suggesting that gabosine D could be a new alternative use for GSH in GST inhibitor design.

Maintaining a simple GST-mediated drug resistance rather than a direct cytotoxic effect (from **24**) is generally a prerequisite for this study. To eliminate a direct cytotoxic effect from GST inhibitor, the effect of **24** was tested on proliferative inhibition against A549 (human lung adenocarcinoma epithelial cell line) and OVCAR-3 (human ovarian carcinoma cell line) cells to identify a suitable concentration for this purpose. As shown in Figure 6, **24** exhibited negligible effect on cell growth inhibition in the range 0−30 μM, suggesting that exclusive GST isozymes inhibition could be achieved with 30 μM **24**.

As a first step toward understanding the effect for the reversal of drug resistance by specifically inhibiting GST isozymes, we evaluated the impact of **24** (0 and 30 μM) on anticancer drugs (cisplatin, oxaliplatin, and doxorubicin) cytotoxicity against A549, in vitro, using MTT assays over a period of 48 h (Table 3). No effects were observed when **24** was incubated with oxaliplatin or doxorubicin. However, a significant enhancement of cisplatin-induced inhibition of cell viability was detected at 30 μM **24**, up to 270% (i.e., decrease in IC_{50} value by 2.7-fold) against A549 (Table 3). Surprisingly, no effects were found in ovarian carcinoma when **24** was incubated with anticancer drugs (Supporting Information Table S1). Collectively, the results demonstrate that **24** specifically enhances the antitumor efficacy of cisplatin in lung cancer cells (not ovarian carcinoma) by blocking GST-mediated drug resistance pathway rather than implicating a direct cytotoxic effect.

Interestingly, **24** has synergetic effect with cisplatin against lung adenocarcinoma epithelial cell line through the inhibition of GSTs. Studies also showed different GST isozymes, GSTA2, GSTM1, and GSTP1-1, to be overexpressed in A549 and OVCAR-3 (Supporting Information Table S2). This raises the question of which GST isozymes are mainly responsible for the resistance to cisplatin. To answer this question, we depleted two GST mRNAs with small interfering RNA (siRNAs) that were specific for GSTM1 and GSTP1-1 genes. To optimize the conditions of RNA interference transfections, proteins levels were quantified by Western blot analyses after treatment (Figure 7). By incorporating si-GSTM1, the viability inhibition of cisplatin was enhanced up to 138% (i.e., decrease in IC_{50} value by 1.4-fold) against A549 (Table 3), suggesting that knockdown of GSTM1 gene is

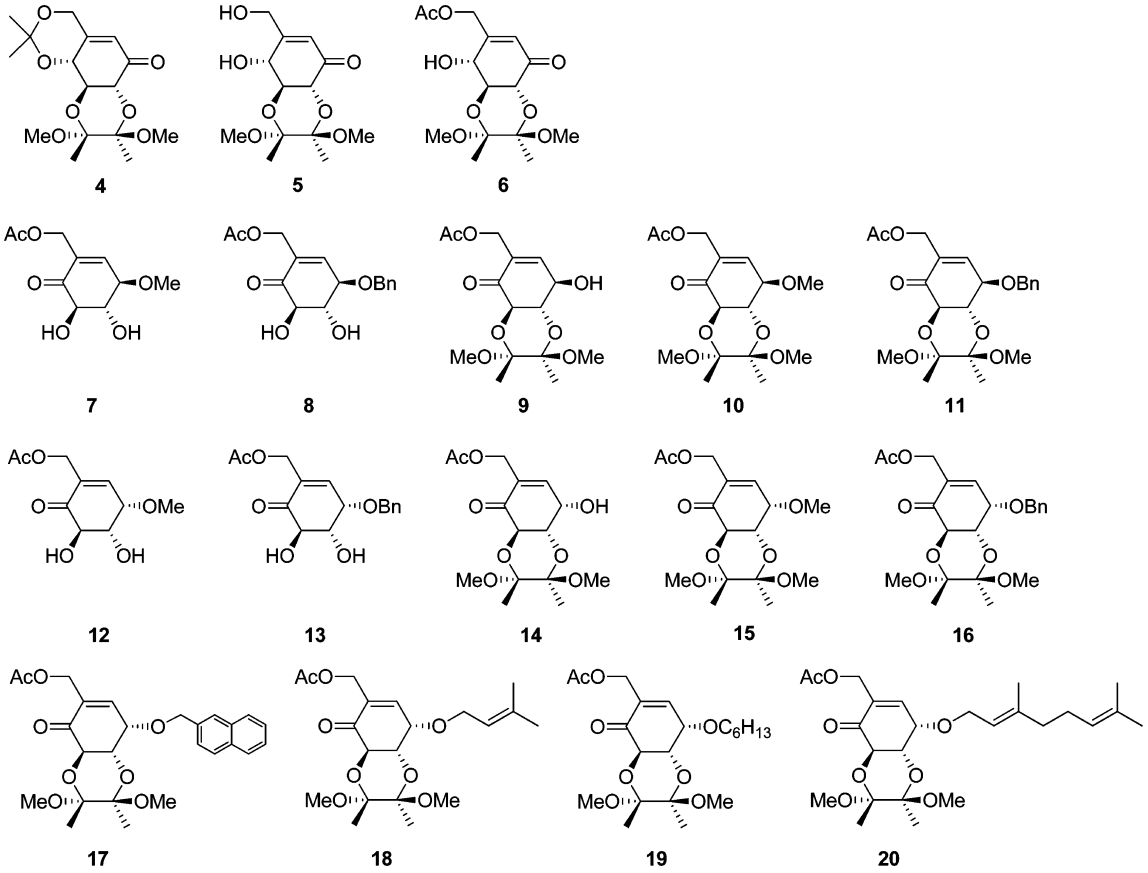

Figure 3. Structures of gabosine analogues **4**–**20**.

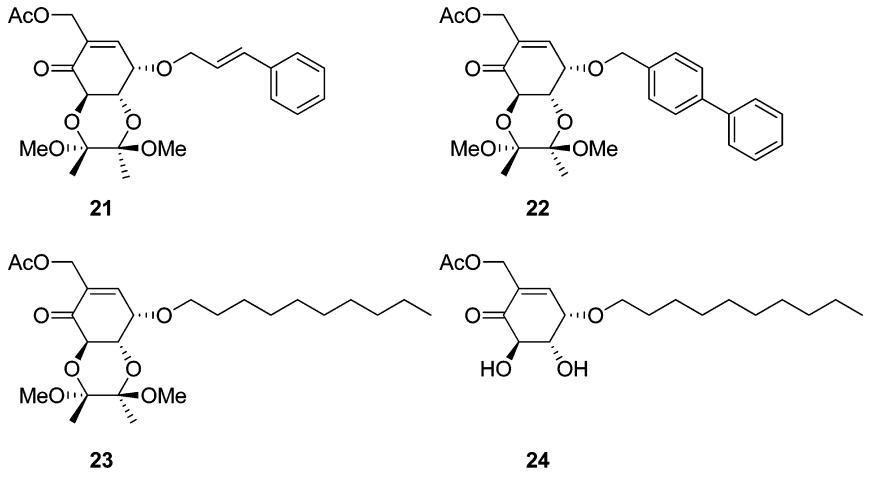

Figure 4. Rational design approach to develop a new class of GSTs inhibitors, gabosine D analogues.

responsible for major enhancement (~50%) of **24**-induced synergetic effect with cisplatin. In contrast, transfection with GSTP1 siRNA for 72 h had no effect on the viability of A549 cells. These results suggest that other minor pathways (e.g., inhibition of other GST isozymes, cellular stress, and downregulation of MRP/P-gp) also play important roles in sensitizing A549 cells to cisplatin-induced death. Neither depletion of GSTP1 nor GSTM1 rendered cells more sensitive to oxaliplatin and doxorubicin, which is apparently consistent with the results shown by **24** (Table 3).

As with GSH, glutathione *S*-transferases contribute crucially to drug resistance by catalyzing adduct formation between GSH and anticancer drugs. In particular, because the expression of μ class of GSTs in COS and HeLa cells enhances cellular resistance to cisplatin,[12] lung, breast, and ovarian cancer patients who are GSTM1-postive generally experience a significant decrease in survival time and rate as compared to the GSTM1-null patients.[13] Our results are in line with the above-mentioned conclusion that inhibition of GSTM1 is essential for overcoming cisplatin resistance in lung cancer A549 cells. However, overwhelming evidence (RNA interference transfections, Table 3) suggests that other factors also play important roles.

dx.doi.org/10.1021/jm201131n | *J. Med. Chem.* 2011, 54, 8574–8581

Table 2. Inhibitory Constants of Gabosine D (3) Analogues 21–24 against Different GST Isozymes[a]

	inhibitory activity, IC_{50} (μM)		
compd	GSTA2	GSTM1	GSTP1-1
21	94.2 ± 4.8	44.5 ± 5.6	58.0 ± 2.5
22	66.3 ± 10.0	44.7 ± 4.9	186.7 ± 18.2
23	33.1 ± 1.4	33.6 ± 2.7	36.5 ± 1.0
24	37.8 ± 2.0	13.4 ± 2.5 (3.2 ± 0.8)[b] (4.7 ± 2.1)[b]	25.3 ± 1.9

[a]Inhibitor concentration at which half-maximal enzyme activity is obtained (IC_{50}, mean ± SEM, n = 3). [b]Values reported are K_i.

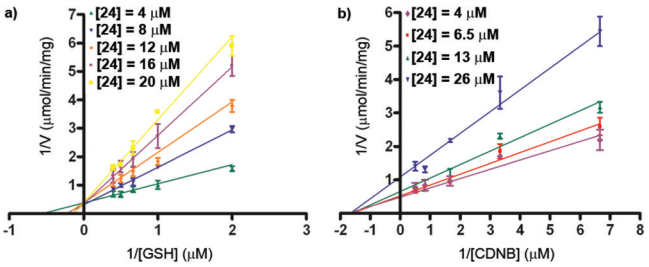

Figure 5. Lineweaver–Burk inhibitory analysis of GSTM1 steady-state kinetics by compound **24**. (a) Reciprocal velocity versus reciprocal GSH concentration with inhibitor **24** (4, 8, 12, 16, 20 μM). CDNB concentration was held constant at 1 mM. (b) Reciprocal velocity versus reciprocal CDNB concentration with inhibitor **24** (4, 6.5, 13, 26 μM). GSH concentration was held constant at 2 mM.

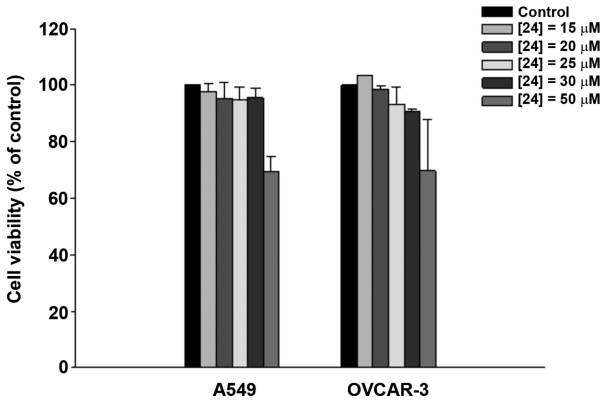

Figure 6. In vitro cell viability effects of compound **24**. Data are representative of three individual experiments, performed in three replicates (IC_{50}, mean ± SEM, n = 3).

CONCLUSION

In summary, we have prepared and identified analogues of natural product gabosine that serve as a new class of human GST inhibitors. The findings highlight the utility of the gabosine moiety for targeting the GSH binding site of GSTs. In particular, the lead **24** shows synergetic effect with cisplatin against lung cancer cell line, A549, through the inhibition of GSTM1. These studies could potentially impact scientific areas for potential development of bioactive compounds to overcome GSTM1-related drug resistance and cellular stress signaling.

EXPERIMENTAL SECTION

General Procedure. Melting points were measured with a Reichert apparatus in Celsius degrees and are uncorrected. Optical rotations were obtained with a Perkin-Elmer model 341 polarimeter, operating at 589 nm. Infrared (IR) spectra were recorded on a Nicolet 205 or a Perkin-Elmer 1600 FT-IR spectrophotometer as thin films on potassium bromide discs. Nuclear magnetic resonance (NMR) spectra were measured with a Bruker DPX300 NMR spectrometer at 300.13 MHz (^{1}H) or 400 MHz (^{1}H) and at 75.47 MHz (^{13}C) or 100 MHz (^{13}C) in $CDCl_3$ solutions, unless stated otherwise. All chemical shifts were recorded in ppm relative to tetramethylsilane (δ = 0.0). Spin–spin coupling constants (J value) recorded in Hz were measured directly from the spectra. MS and HRMS were measured on a ThermoFinnigan MAT 95 KL at the Department of Chemistry, The Chinese University of Hong Kong. All reactions were monitored by analytical thin-layer chromatography (TLC) on Merck aluminum-precoated plates of silica gel 60 F254 with detection by spraying with 5% (w/v) dodecamolybdophosphoric acid in ethanol or 5% (w/v) ninhydrin in ethanol and subsequent heating. E. Merck silica gel 60 (230–400 mesh) was used for flash chromatography. All reagents and solvents were general reagent grade unless otherwise stated. THF was freshly distilled from Na/benzophenone ketyl under nitrogen. Dichloromethane was freshly distilled from P_2O_5 under nitrogen. Other reagents were purchased from commercial suppliers and were used without purification. Analytical HPLC was performed as follows: eluent = MeOH: H_2O (1:1); flow rate = 1.0 mL/min; Alltima C18 5 μ 250 mm × 4.6 mm column; detection at 254 nm. The purity of all the final gabosine analogues **1**–**24** was established as being >95% by ^{1}H NMR and HPLC analysis.

Synthesis of 28i (R = Decyl). Sodium hydride (60%, 69.2 mg, 1.73 mmol) was suspended in dry THF (5 mL) under nitrogen at 0 °C. A solution of the α-alcohol **26** (119.6 mg, 0.36 mmol) in THF (5 mL) was added dropwise over 1 h at 0 °C, and then the mixture was stirred for 1 h at 0 °C. 1-Bromodecane (0.23 mL, 1.11 mmol) was added dropwise over 15 min, and tetra-*n*-butylammomium iodide (2.67 mg, 0.067 mmol) was then added. The reaction mixture was heated at reflux at for 1 h. After cooling to room temperature, water was added slowly at 0 °C to destroy the excess of hydride, and this was followed by the addition of saturated NH_4Cl solution. The aqueous

Table 3. Synergetic Effects of 4-*O*-Decyl-Gabosine D (24), GSTP1si and GSTM1si on Cell Viability of Human Lung Cancer Cell Line A549[a]

	IC_{50} (μM)[b]			
drug	control	30 μM [**24**]	GSTP1si	GSTM1si
cisplatin	32.3 ± 3.9	12.0 ± 1.1	38.3 ± 1.0	23.4 ± 1.2
oxaliplatin	59.5 ± 1.7	55.2 ± 5.9	56.4 ± 3.6	58.3 ± 3.4
doxorubicin	0.51 ± 0.06	0.64 ± 0.04	0.65 ± 0.12	0.52 ± 0.03

[a]A dose-dependent inhibitory effect on cell growth was observed and respective IC_{50} values of cisplatin, oxaliplatin, and doxorubicin were determined after 48 h. For example, IC_{50} values of cisplatin were obtained in the absence (IC_{50} = 32.3 μM) or presence (IC_{50} = 12.0 μM) of 30 μM 4-*O*-decyl-gabosine D (**24**). This means that the presence of **24** reduces the dosage of cisplatin and enhances the efficacy of cisplatin to inhibit the same amount of cancer cells growth. The calculation of 270% (2.7 × 100%) was derived from 2.7-fold increase of IC_{50} values from 32.3 μM to 12.0 μM (32.3/12.0 = 2.7). [b]Cell proliferation was determined by measuring the absorbance 540 nm (MTT assay). Data are representative of three individual experiments, performed in three replicates (IC_{50}, mean ± SEM, n = 3).

dx.doi.org/10.1021/jm201131n | J. Med. Chem. 2011, 54, 8574–8581

Figure 7. Conditions of depletion of GSTP1 and GSTM1 after treatment with siRNA for 48 and 72 h in A549 cells. Expression levels of GSTP1 (a) and GSTM1 (b) proteins were quantified by Western blot analysis.

layer was extracted with Et_2O (3 × 100 mL). The combined organic extracts were washed with brine, dried over $MgSO_4$, and filtered. Concentration of the filtrate followed by flash chromatography (hexane:-dichloromethane, 1:5) gave decyl ether **28i** (127 mg, 75%) as a colorless oil: $[\alpha]_D^{20}$ −72.6 (*c* 1.98, $CHCl_3$); R_f 0.4 (hexane:Et_2O, 1:1). IR (thin film) 2992, 2926, 1462, 1374, 1199, 1091, 852 cm^{-1}. ^1H NMR (300 MHz, $CDCl_3$) δ 0.86 (3H, t, *J* = 6 Hz), 1.25 (14H, m), 1.29 (3H, s), 1.30 (3H, s), 1.36 (3H, s), 1.48 (3H, s), 1.51−1.59 (2H, m), 3.25 (3H, s), 3.26 (3H, s), 3.47−3.57 (1H, dt, *J* = 9, 6 Hz), 3.62 (1H, dd, *J* = 11.1, 3.9 Hz), 3.79−3.88 (2H, m), 4.07 (1H, d, *J* = 8.1 Hz), 4.13 (1H, d, *J* = 4.2 Hz), 4.34−4.35 (1H, m), 4.38 (1H, d, *J* = 9 Hz), 5.51 (1H, d, *J* = 4.8 Hz). ^{13}C NMR (75.47 MHz, $CDCl_3$) δ 14.5, 18.1, 18.2, 20.7, 23.1, 26.5, 28.4, 29.8, 30.0, 30.1, 30.7, 32.3, 48.3, 48.4, 63.3, 67.8, 69.5, 70.7, 72.3, 73.2, 98.9, 99.4, 99.5, 119.3 135.5. MS (ESI) *m*/*z* (relative intensity) 493 ([M + Na]$^+$, 100). HRMS (ESI) calcd for $C_{26}H_{46}O_7$ [M + Na]$^+$ 493.3136, found 493.3119.

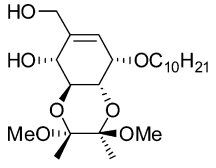

33i

Synthesis of 33i. A solution of the alkyl ether **28i** (189.9 mg, 0.40 mmol) in 80% aqueous AcOH (4.5 mL) was stirred at room temperature for 1.5 h. The solvent was removed under reduced pressure, and the residue was purified by flash chromatography (hexane:EtOAc, 1:1) to afford diol **33i** (150.5 mg, 87%) as a colorless oil: $[\alpha]_D^{20}$ −53.7 (*c* 1.29, $CHCl_3$); R_f 0.47 (EtOAc). IR (thin film) 3419, 2925, 1650, 1463, 1375, 1123, 885 cm^{-1}. ^1H NMR (300 MHz, $CDCl_3$) δ 0.86 (3H, t, *J* = 6.6 Hz), 1.25−1.31 (20H, m), 1.44−1.63 (2H, m), 2.73 (1H, brs), 3.07 (1H, d, *J* = 5.4 Hz), 3.24 (3H, s), 3.28 (3H, s), 3.48−3.59 (2H, m), 3.80−3.94 (2H, m), 4.06 (1H, dd, *J* = 11.1, 8.1 Hz), 4.16−4.28 (3H, m), 5.79 (1H, d, *J* = 5.4 Hz). ^{13}C NMR (75.47 MHz, $CDCl_3$) δ 14.5, 18.1, 18.2, 23.1, 26.5, 29.8, 30.0, 30.1, 30.7, 32.3, 48.2, 48.3, 64.1, 69.5, 70.4, 72.0, 72.4, 73.0, 99.1, 99.4, 122.6, 141.7. MS (ESI) *m*/*z* (relative intensity) 453 ([M + Na]$^+$, 100). HRMS (ESI) calcd for $C_{23}H_{42}O_7$ [M + Na]$^+$ 453.2823, found 453.2834.

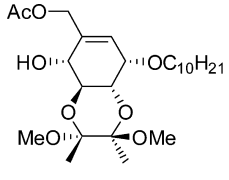

34i

Synthesis of 34i. To a solution of the diol **33i** (121.7 mg, 0.28 mmol) and 2,4,6-collidine (0.11 mL, 0.83 mmol) in dry CH_2Cl_2 (10 mL) at −78 °C was added acetyl chloride (AcCl) (28 μL, 0.39 mmol) slowly. The reaction mixture was stirred for 15 h at −78 °C and quenched with water (5 mL). The resultant solution was allowed to warm to room temperature. The aqueous phase was extracted with EtOAc (3 × 20 mL). The combined organic extracts were then washed with cold 1N HCl (2 × 10 mL), cold DI water (10 mL). and cold diluted $NaHCO_3$ (10 mL). The organic layer was washed with brine (2 × 10 mL), dried ($MgSO_4$), and filtered. Concentration of the filtrate followed by flash chromatography (hexane:EtOAc, 2:1) gave acetate **34i** (102.3 mg, 89%) as a colorless oil: $[\alpha]_D^{20}$ −52.4 (*c* 0.57, $CHCl_3$); R_f 0.52 (hexane:EtOAc, 1:1). IR (thin film) 3481, 2925, 1744, 1458, 1374, 1232, 1124, 885 cm^{-1}. ^1H NMR (300 MHz, $CDCl_3$) δ 0.87 (3H, t, *J* = 6.9 Hz), 1.26 (14H, m), 1.30 (3H, s), 1.32 (3H, s), 1.54−1.57 (2H, m), 2.06 (3H, s), 2.62 (1H, d, *J* = 4.8 Hz), 3.25 (3H, s), 3.29 (3H, s), 3.50−3.57 (1H, dt, *J* = 9, 6 Hz), 3.60 (1H, dd, *J* = 11.1, 3.9 Hz), 3.81−3.87 (1H, m), 3.91, (1H, dd, *J* = 5.4, 3.9 Hz), 4.09 (1H, dd, *J* = 10.8, 8.1 Hz), 4.18−4.21 (1H, m), 4.50 (1H, d, *J* = 12.9 Hz), 4.88 (1H, d, *J* = 12.9 Hz), 5.87 (1H, d, *J* = 5.1 Hz). ^{13}C NMR (75.47 MHz, $CDCl_3$) δ 14.5, 18.1, 18.2, 21.3, 23.1, 26.5, 29.8, 30.0, 30.1, 30.2, 30.7, 32.3, 48.3, 48.4, 64.4, 69.4, 70.2, 70.7, 72.4, 72.5, 99.2, 99.5, 125.5, 137.9, 171.4. MS (ESI) *m*/*z* (relative intensity) 495 ([M + Na]$^+$, 100). HRMS (ESI) calcd for $C_{25}H_{44}O_8$ [M + Na]$^+$ 495.2928, found 495.2931.

Synthesis of 23. A mixture of 3 Å molecular sieves (ca. 100 mg) and pyridinium dichromate (PDC) (122.4 mg, 0.33 mmol) was added to a solution of the acetate **34i** (353.4 mg, 0.75 mmol) in dry CH_2Cl_2 (30 mL) under N_2 at 0 °C. The mixture was stirred for 20 h at room temperature. The mixture was then filtered through a pad of Celite. and the residue was washed with EtOAc until no product was observed in the eluent (checked with TLC). Concentration of the filtrate followed by flash chromatography (hexane:Et_2O, 2:1) yielded enone **23** (348.8 mg, 99%) as a colorless oil; $[\alpha]_D^{20}$ −17.1 (*c* 2.49, $CHCl_3$); R_f 0.37 (hexane:Et_2O, 1:2). IR (thin film) 2926, 2855, 1748, 1461, 1376, 1139, 950 cm^{-1}. ^1H NMR (300 MHz, $CDCl_3$) δ 0.86 (3H, t, *J* = 6.9 Hz), 1.25−1.31 (17H, m), 1.37 (3H, s), 1.53−1.64 (2H, m), 2.07 (3H, s), 3.23 (3H, s), 3.28 (3H, s), 3.58−3.65 (1H, dt, *J* = 9, 6.3 Hz), 3.92−4.01 (2H, m), 4.18 (1H, dd, *J* = 6, 3.3 Hz), 4.70 (1H, dd, *J* = 14.1, 1.2 Hz), 4.77−4.82 (2H, m), 6.85 (1H, d, *J* = 6.3 Hz). ^{13}C NMR (75.47 MHz, $CDCl_3$) δ 14.5, 18.1, 21.3, 23.1, 26.5, 29.8, 29.9, 30.0, 30.1, 30.7, 32.3, 48.4, 48.7, 62.0, 69.9, 70.1, 72.2, 72.1, 99.7, 100.2, 135.6, 140.0, 170.8, 193.5. MS (ESI) *m*/*z* (relative intensity) 493 ([M + Na]$^+$, 100). HRMS (ESI) calcd for $C_{25}H_{42}O_8$ [M + Na]$^+$ 493.2772, found 493.2780.

Synthesis of 24. To a solution of the enone **23** (7.5 mg, 0.016 mmol) in CH_2Cl_2 (5 mL) were added trifluoroacetic acid (TFA) (0.1 mL) and H_2O (0.01 mL), and the mixture was stirred at room temperature for 3 h. The solvent was removed under reduced pressure and flash chromatography (hexane:EtOAc, 1:2) of the residue afforded diol **24** (5 mg, 88%) as a white solid: mp 47.8−48.2 °C; $[\alpha]_D^{20}$ +114 (*c* 0.21, $CHCl_3$); R_f 0.5 (EtOAc). IR (thin film) 3417, 2924, 2854, 1747, 1692, 1369, 1228, 1102 cm^{-1}. ^1H NMR (300 MHz, CD_3OD) δ 0.90 (3H, t, *J* = 6.9 Hz), 1.29 (14H, m), 1.58−1.67 (2H, m), 2.07 (3H, s), 3.65 (1H, dt, *J* = 9.3, 6.6 Hz), 3.66 (1H, dt, *J* = 9.3, 6.6 Hz), 3.90 (1H, dd, *J* = 9.3, 3.9 Hz), 4.26 (1H, dd, *J* = 4.8, 3.9 Hz), 4.31 (1H, d, *J* = 9.3 Hz), 4.74 (2H, s), 7.02−7.048 (1H, dt, *J* = 4.8, 1.5 Hz). ^{13}C NMR (75.47 MHz, CD_3OD) δ 14.4, 20.6, 23.7, 27.1, 30.4, 30.6, 30.7, 31.1, 33.0, 61.6, 72.3, 73.6, 75.1, 75.3, 135.4, 143.8, 172.1, 198.5. MS (ESI) *m*/*z* (relative intensity) 379 ([M + Na]$^+$, 100). HRMS (ESI) calcd for $C_{19}H_{32}O_6$ [M + Na]$^+$ 379.2091, found 379.2098. HPLC analysis indicated that it is free of any diastereomer and purity was determined to be ≥95%.

Cell Lines. Human lung cancer A549 cells (BCRC 60074) and ovarian carcinoma OVCAR-3 cells (BCRC 60551) were purchased from the Food Industry Research and Development Institute (Hsinchu, Taiwan). The cells were grown in DMEM medium

dx.doi.org/10.1021/jm201131n | *J. Med. Chem.* 2011, 54, 8574−8581

containing 10% (v/v) FBS, 1.5 g/L $NaHCO_3$, 5 mM HEPES, 1 mM sodium pyruvate, or RPMI1640 medium containing 20% (v/v) FBS, 1.5 g/L $NaHCO_3$, 4.5 g/L glucose, 10 mM HEPES, 1 mM sodium pyruvate, and supplemented with 0.01 mg/mL bovine insulin in a humidified incubator under 5% CO_2 and 95% air at 37 °C.

Gabosine Analogue Inhibitory Effect on Cell Viability. Cell proliferation was determined using [3-(4,5-dimethylthiazol-2-yl)-2,5-diphenyl-tetrazolium bromide] (MTT) assay. Briefly, the cells were cultured in 96-well plates at 4×10^3 cells/well in DMEM or RPMI1640 for 24 h. Then, the cells were treated with compound **24** (30 μM) for 2 h, followed by adding various concentrations of anticancer drugs (cisplatin, oxaliplatin, and doxorubicin) for 48 h. After incubation, the medium was removed and cells were washed with PBS, followed by incubating with MTT solution for 4 h. The medium was removed, and the formazan was solubilized in DMSO and measured spectrophotometrically at 570 nm. The percentage of viable cells was estimated by comparing with untreated control cells.

Transient Transfection of siRNA against GSTP1 and GSTM1. The plasmid containing siRNA against GSTP1 and GSTM1 (GSTP1si and GSTP1si; Stealth RNAi) and Lipofectamine RNAiMAX transfection reagent were purchased from invitrogen (Australia). GSTP1si and GSTM1si stock solutions (20 μM) were diluted with DEPC water to form 10 μM solutions. Lipofectamine RNAiMAX transfection reagent was mixed with 10 μM GSTP1si or GSTM1si incubated for 20 min. The final concentration of siRNA was 10 nM. The cells were incubated with GSTP1si and GSTM1si for 48 and 72 h.

Western Blotting. Cancer cells were lysed in lysis buffer (iNtRON BIOTECHNOLOGY), followed by centrifugation for 30 min at 4 °C. The protein (20 μg) from the supernatant were separated on SDS-polyacrylamide gel electrophoresis and transferred to PVDF membrane. After blocking with TBS buffer (20 mM Tris–HCl, 150 mM NaCl, pH 7.4) containing 5% nonfat milk, the membrane was incubated with GSTP1, GSTM1, and actin antibody overnight and then incubated with horseradish peroxidase-conjugated antirabbit or antimouse IgG for 1 h, followed by visualization using an ECL chemiluminescent detection kit (Amersham Co, Bucks, UK).

Data Analysis. Data were expressed as mean ± standard deviation (mean ± SD) and analyzed with *t*-test. If *P* was less than 0.05, differences were considered statistically significant.

Cloning, Expression, and Purification of Human GSTM1. Human GSTM1 was cloned, expressed, and purified by using the previously described procedures.[7d] The resulting hGSTM1 was added 20% glycerol before storage at −80 °C.

Expression and Purification of Human GSTA2. Human GSTA2 was cloned, expressed, and purified by using the previously described procedures and stored in 16% glycerol at −80 °C.[7c]

Human GST Activity. Human GST activity was determined spectrophotometrically at 340 nm and according to the procedure of Habig et al..[14]

Inhibition of Human GST Isoenzymes-IC_{50} and K_i Determinations. Human GST M1 (32 ng) was incubated with inhibitor (ranging from 0 to 200 μM) in 100 mM potassium phosphate buffer pH 6.5 at 37 °C. The reaction was initiated with GSH (final 2 mM) and monitored at 340 nm in a period of 3 min. IC_{50} values were then calculated by nonlinear regression analysis of inhibition data.

Lineweaver–Burk inhibitory analyses were performed in the same condition as GST inhibition assays. GST M1 steady-state kinetics by inhibitor **24** was assayed with various concentration of compound **24** at either constant CDNB (1 mM) or constant GSH (2 mM) concentrations. Lineweaver–Burk plots were plotted with reciprocal velocity against reciprocal GSH/CDNB concentration, and the corresponding K_i values were calculated by fitting inhibition data with competitive/noncompetitive inhibition equations.

■ ASSOCIATED CONTENT

Ⓢ Supporting Information

Cytotoxicity, experimental procedures, compound characterization, and NMR spectra. This material is available free of charge via the Internet at http://pubs.acs.org.

■ AUTHOR INFORMATION

Corresponding Author

*For T.K.M.S.: phone, +852-2609 6344; fax, +852 2603-5057; E-mail, tonyshing@cuhk.edu.hk (synthesis). For W.S.L.: phone, +886 (2) 27898662; fax, +886 (2) 27831237; E-mail, wenshan@chem.sinica.edu.tw.

■ ACKNOWLEDGMENTS

We are grateful for funding from Academia Sinica and the National Science Council. This work was also supported by a Strategic Investment Scheme administered by the Center of Novel Functional Molecules and by a direct grant from The Chinese University of Hong Kong.

■ ABBREVIATIONS USED

hGSTs, human glutathione *S*-transferases; MRP, multidrug-resistance-related proteins; P-gp, P-glycoprotein; PDC, pyridinium dichromate; GSH, glutathione; A549, human lung adenocarcinoma epithelial cell line; OVCAR-3, human ovarian carcinoma cell line; siRNA, small interfering RNA

■ REFERENCES

(1) (a) Tew, K. D. Glutathione-Associated Enzymes in Anticancer Drug Resistance. *Cancer Res.* **1994**, *54*, 4313–4320. (b) Ang, W. H.; Khalaila, I.; Allardyce, C. S.; Juillerat-Jeanneret, L.; Dyson, P. J. Rational Design of Platinum(IV) Compounds to Overcome Glutathione-*S*-Transferase Mediated Drug Resistance. *J. Am. Chem. Soc.* **2005**, *127*, 1382–1383.

(2) Broxterman, H. J.; Giaccone, G.; Lankelma, J. Multidrug Resistance Proteins and Other Drug Transport-Related Resistance to Natural Product Agents. *Curr. Opin. Oncol.* **1995**, *7*, 532–540.

(3) (a) Hayes, J. D.; Pulford, D. J. The Glutathione *S*-Transferase Supergene Family: Regulation of GST and the Contribution of the Isoenzymes to Cancer Chemoprotection and Drug Resistance. *Crit. Rev. Biochem. Mol. Biol.* **1995**, *30*, 445–600. (b) Townsend, D. M.; Tew, K. D. The role of Glutathione-*S*-Transferase in Anti-Cancer Drug Resistance. *Oncogene* **2003**, *22*, 7369–7375.

(4) Nebert, D. W.; Vasiliou, V. Analysis of the Glutathione *S*-Transferase (GST) Gene Family. *Hum. Genomics* **2004**, *1*, 460–464.

(5) (a) McIlwain, C. C.; Townsend, D. M.; Tew, K. D. Glutathione *S*-Transferase Polymorphisms: Cancer Incidence and Therapy. *Oncogene* **2006**, *25*, 1639–1648. (b) Lo, H. W.; Ali-Osman, F. Genetic Polymorphism and Function of Glutathione *S*-Transferases in Tumor Drug Resistance. *Curr. Opin. Pharmacol.* **2007**, *7*, 367–374.

(6) (a) Wu, Z.; Minhas, G. S.; Wen, D.; Jiang, H.; Chen, K.; Zimniak, P.; Zheng, J. Design, Synthesis, and Structure–Activity Relationships of Haloenol Lactones: Site-Directed and Isozyme-Selective Glutathione *S*-Transferase Inhibitors. *J. Med. Chem.* **2004**, *47*, 3282–3294. (b) Ricci, G.; De Maria, F.; Antonini, G.; Turella, P.; Bullo, A.; Stella, L.; Filomeni, G.; Federici, G.; Caccuri., A. M. 7-Nitro-2,1,3-Benzoxadiazole Derivatives, a New Class of Suicide Inhibitors for Glutathione *S*-Transferases. Mechanism of Action of Potential Anticancer Drugs. *J. Biol. Chem.* **2005**, *280*, 26397–26405. (c) Ang, W. H.; Parker, L. J.; De Luca, A.; Juillerat-Jeanneret, L.; Morton, C. J.; Lo Bello, M.; Parker, M. W.; Dyson, P. J. Rational Design of an Organometallic Glutathione Transferase Inhibitor. *Angew. Chem., Int. Ed. Engl.* **2009**, *48*, 3854–3857.

(7) (a) Lyttle, M. H.; Hocker, M. D.; Hui, H. C.; Caldwell, C. G.; Aaron, D. T.; Engqvist-Goldstein, A.; Flatgaard, J. E.; Bauer, K. E.

Isozyme-Specific Glutathione-*S*-Transferase Inhibitors: Design and Synthesis. *J. Med. Chem.* **1994**, *37*, 189−194. (b) Jao, S. C.; Chen, J.; Yang, K.; Li, W. S. Design of Potent Inhibitors for *Schistosoma Japonica* Glutathione *S*-Transferase. *Bioorg. Med. Chem.* **2006**, *14*, 304−318. (c) Lo, W. J.; Chiou, Y. C.; Hsu, Y. T.; Lam, W. S.; Chang, M. Y.; Jao, S. C.; Li, W. S. Enzymatic and Nonenzymatic Synthesis of Glutathione Conjugates: Application to the Understanding of a Parasite's Defense System and Alternative to the Discovery of Potent Glutathione *S*-Transferase Inhibitors. *Bioconjugate Chem.* **2007**, *18*, 109−120. (d) Li, W. S.; Lam, W. S.; Liu, K. C.; Wang, C. H.; Chang, H. C.; Jen, Y. C.; Hsu, Y. T.; Shivatare, S. S.; Jao, S. C. Overcoming the Drug Resistance in Breast Cancer Cells by Rational Design of Efficient Glutathione *S*-Transferase Inhibitors. *Org. Lett.* **2010**, *12*, 20−23.

(8) Tatsuta, K.; Tsuchiya, T.; Mikami, N.; Umezawa, S.; Umezawa, H.; Naganawa, H. KD16-U1, a New Metabolite of Streptomyces: Isolation and Structural Studies. *J. Antibiot.* **1974**, *27*, 579−586.

(9) (a) Shing, T. K. M.; Cheng, H. M. Short Syntheses of Gabosine I and Gabosine G from delta-D-Gluconolactone. *J. Org. Chem.* **2007**, *72*, 6610−6613. (b) Shing, T. K. M.; Cheng, H. M. Facile Syntheses of (+)-Gabosines A, D, and E. *Org. Biomol. Chem.* **2009**, *7*, 5098−5102. (c) Shing, T. K. M.; Cheng, H. M.; Wong, W. F.; Kwong, C. S. K.; Li, J.; Lau, C. B. S.; Leung, P. S.; Cheng, C. H. K. Enantiospecific Synthesis of Pseudoacarviosin as a Potential Antidiabetic Agent. *Org. Lett.* **2008**, *10*, 3145−3148. (d) Shing, T. K. M.; So, K. H.; Kwok, W. S. Carbocyclization of Carbohydrates: Diastereoselective Synthesis of (+)-Gabosine F, (−)-Gabosine O, and (+)-4-*Epi*-gabosine O. *Org. Lett.* **2009**, *11*, 5070−5073.

(10) (a) Huntley, C. F. M.; Hamilton, D. S.; Creighton, D. J.; Ganem, B. Reaction of COTC with Glutathione: Structure of the Putative Glyoxalase I Inhibitor. *Org. Lett.* **2000**, *2*, 3143−3144. (b) Kamiya, D.; Uchihata, Y.; Ichikawa, E.; Kato, K.; Umezawa, K. Reversal of Anticancer Drug Resistance by COTC Based on Intracellular Glutathione and Glyoxalase I. *Bioorg. Med. Chem. Lett.* **2005**, *15*, 1111−1114.

(11) Burg, D.; Riepsaame, J.; Pont, C.; Mulder, G.; van de Water, B. Peptide-Bond Modified Glutathione Conjugate Analogs Modulate GSTπ Function in GSH-Conjugation, Drug Sensitivity and JNK Signaling. *Biochem. Pharmacol.* **2006**, *71*, 268−277.

(12) (a) Puchalski, R. B.; Fahl, W. E. Expression of Recombinant Glutathione *S*-Transferase pi, Ya, or Yb1 Confers Resistance to Alkylating Agents. *Proc. Natl. Acad. Sci. U.S.A.* **1990**, *87*, 2443−2447. (b) Hao, X. Y.; Widersten, M.; Ridderström, M.; Hellman, U.; Mannervik, B. Co-Variation of Glutathione Transferase Expression and Cytostatic Drug Resistance in HeLa Cells: Establishment of Class Mu Glutathione Transferase M3-3 as the Dominating Isoenzyme. *Biochem. J.* **1994**, *297*, 59−67.

(13) (a) Ge, H.; Lam, W. K.; Lee, J.; Wong, M. P.; Yew, W. W.; Lung, M. L. Analysis of L-Myc and GSTM1 Genotypes in Chinese Non-Small Cell Lung Carcinoma Patients. *Lung Cancer* **1996**, *15*, 355−366. (b) Nedelcheva, K. V.; Andersen, T. I.; Erikstein, B.; Geitvik, G.; Skovlund, E.; Nesland, J. M.; Børresen-Dale, A. L. Single Tube Multiplex Polymerase Chain Reaction Genotype Analysis of GSTM1, GSTT1 and GSTP1: Relation of Genotypes to TP53 Tumor Status and Clinicopathological Variables in Breast Cancer Patients. *Pharmacogenetics* **1998**, *8*, 441−447. (c) Yang, P.; Yokomizo, A.; Tazelaar, H. D.; Marks, R. S.; Lesnick, T. G.; Miller, D. L.; Sloan, J. A.; Edell, E. S.; Meyer, R. L.; Jett, J.; Liu, W. Genetic Determinants of Lung Cancer Short-Term Survival: The Role of Glutathione-Related Genes. *Lung Cancer* **2002**, *35*, 221−229. (d) Matsumoto, T.; Hayase, R.; Kodama, J.; Kamimura, S.; Yoshinouchi, M.; Kudo, T. Immunohistochemical Analysis of Glutathione *S*-Transferase in Expression in Ovarian Tumors. *Eur. J. Obstet. Gynecol. Reprod. Biol.* **1997**, *73*, 171−176. (e) Medeiros, R.; Pereira, D.; Afonso, N.; Palmeira, C.; Faleiro, C.; Afonso-Lopes, C.; Freitas-Silva, M.; Vasconcelos, A.; Costa, S.; Osório, T.; Lopes, C. Platinum/Paclitaxel-Based Chemotherapy in Advanced Ovarian Carcinoma: Glutathione *S*-Transferase Genetic Polymorphisms as Predictive Biomarkers of Disease Outcome. *Int. J. Clin. Oncol.* **2003**, *8*, 156−161.

(14) Habig, W. H.; Jakoby, W. B. Assays for Determination of Glutathione *S*-transferase. *Methods Enzymol.* **1981**, *77*, 398−405.